Discrete W Transform Based Index-Keying M-ary DCSK for Non-coherent Chaotic Communications

Xiangming Cai, Weikai Xu, *Member, IEEE,* Shaohua Hong, *Member, IEEE,* Lin Wang, *Senior Member, IEEE*

***Abstract*—In this letter, a non-coherent discrete W transform based index-keying M-ary differential chaos shift keying (DWT-IK-MDCSK) system is proposed to tackle the high peak to average power ratio (PAPR) in the code-shifted DCSK systems and meet the demand of high-data-rate transmissions. In such system, multiple chaotic signals and their Hilbert transforms are cooperated closely to convey the M-ary information-bearing signals, and the resultant signals are extended by the index-keying discrete W vectors prior to being added up and transmitted over the channel. Since the index keying technique is used to select the specific discrete W vectors, extra information bits are conveyed by the indices of these vectors, thereby improving the data rate. Then, the analytical bit error rate (BER) expressions of DWT-IK-MDCSK are derived over additive white Gaussian noise (AWGN) and multipath Rayleigh fading channels. Finally, simulation results show the DWT-IK-MDCSK system has a lower PAPR and better BER performance compared to its competitors.**

***Index Terms*—Non-coherent communications, discrete W transform, index keying, differential chaos shift keying.**

I. Introduction

The upcoming Internet of Things (IoTs) and 5G communications are expected to support high-data-rate and energy-efficient wireless devices [1]. Traditional coherent communications need the channel state information (CSI) to recover information bits, which introduces a great number of system overheads. In contrast, non-coherent communications, built with the simple transmitted-reference (TR) signaling and auto-correlation receiver (AcR), offer a low-complexity solution for IoT devices. Consequently, there has been a compelling interest to study the non-coherent communications [2].

A non-coherent differential chaos shift keying (DCSK) system [3] has the ability to resist multipath fading without being bound by chaos synchronization [4]. However, half of the DCSK symbol duration is used to transmit the reference signal, causing a low data rate [5]. To tackle this problem, an M-ary DCSK [6] system allows multiple information bits to be modulated into the information-bearing signal. Then the multilevel code-shifted M-ary DCSK (MCS-MDCSK) [7] and discrete cosine spreading aided M-ary DCSK (DCS-MDCSK) [8] systems were proposed to achieve the high-data-rate transmission with the aid of Walsh and discrete cosine codes, respectively.

As an innovative way to convey information in an energy-efficient manner, the code index modulation (CIM) technique was proposed in [9] and further developed in [10] to support multiple-input multiple-output (MIMO). In addition, a CIM-based spread-spectrum framework was proposed in [11] to get the superior BER performance. However, CSI is necessary for these schemes so that their applications are limited. To cancel the need for CSI, a single-carrier CIM-based multilevel code-shifted DCSK (CIM-MCS-DCSK) system was proposed in [12]. Then a CIM-based multicarrier M-ary DCSK (CIM-MC-MDCSK) system was proposed in [13], [14].

However, in the code-shifted DCSK systems [7], [8], the reference and information-bearing signals are overlapped together prior to being transmitted, and therefore the instantaneous power of the transmitted signals will be more than the average power, finally resulting in a high peak to average power ratio (PAPR). On the other hand, the traditional CIM [9], [10], [13], [14] is based on the Walsh codes whose order must be the power of two and it restricts both flexibility and practicality.

To address these issues, we propose a non-coherent discrete W transform based index-keying M-ary differential chaos shift keying (DWT-IK-MDCSK) system, where only parts of discrete W vectors are selected via the index keying and the indices of these vectors are regarded as an additional dimension to improve the data rate. The analytical BERs of DWT-IK-MDCSK are derived over the additive white Gaussian noise (AWGN) and multipath fading channels. Simulations show the DWT-IK-MDCSK system has higher data rate, lower PAPR and better BER performance compared to its competitors.

The remainder of this paper is organized as follows: Section II shows the principle of the proposed system. The performance analysis and simulation results are given in Sections III and IV, respectively. Section V concludes this paper.

II. System Model

Fig. 1 depicts the DWT-IK-MDCSK system model. The logistic map, $c_{\ell+1} = 1 - 2c_\ell^2, \ell = 1, 2, \cdots$, with U different initial values is used to produce U chaotic signals, $\{\mathbf{c}_j\}_{j=1}^{U} = \{\mathbf{c}_1, \mathbf{c}_2, \cdots, \mathbf{c}_U\}$, where $\mathbf{c}_j = [c_{j,1}, c_{j,2}, \cdots, c_{j,\beta}]$ is a β-length chaotic signal. The resultant signals are processed by the Gram-Schmidt algorithm to obtain their orthonormal

This work was supported in part by the National Natural Science Foundation of China under Grant 61671395 and Grant 61871337, the Natural Science Foundation of Fujian Province (No. 2020J01003) and the Natural Science Foundation of Guangdong Province (No. 2018A030313710).

Xiangming Cai, Weikai Xu, and Lin Wang are with the Department of Information and Communication Engineering, Xiamen University, Xiamen 361005, China (e-mail: samson0102@qq.com; xweikai@xmu.edu.cn; wanglin@xmu.edu.cn).

Shaohua Hong is with the Department of Information and Communication Engineering, Xiamen University, Xiamen 361005, China, and also with the Shenzhen Research Institute of Xiamen University, Shenzhen 518000, China (e-mail: hongsh@xmu.edu.cn).

This article has been accepted for publication in a future issue of this journal, but has not been fully edited. Content may change prior to final publication. Citation information: DOI 10.1109/LCOMM.2021.3095075, IEEE Communications Letters

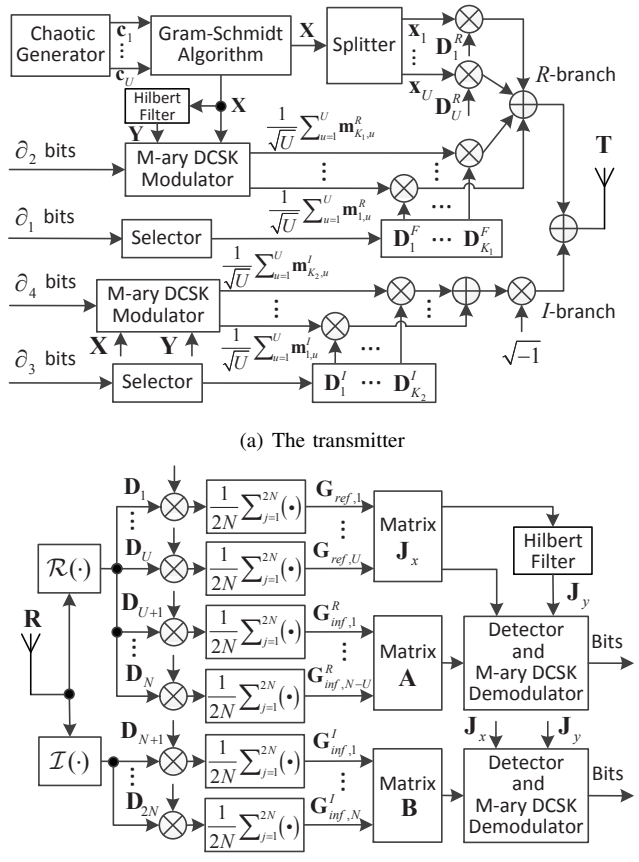

(a) The transmitter

(b) The receiver

Fig. 1. Block diagram of the DWT-IK-MDCSK system.

versions, formulated as

$$\mathbf{x}_u = \begin{cases} \frac{\mathbf{c}_1}{\|\mathbf{c}_1\|_2}, & u = 1, \\ \frac{\mathbf{c}_u - \sum_{k=1}^{u-1} \frac{\langle \mathbf{c}_u, \mathbf{x}_k \rangle}{\langle \mathbf{x}_k, \mathbf{x}_k \rangle} \mathbf{x}_k}{\left\| \mathbf{c}_u - \sum_{k=1}^{u-1} \frac{\langle \mathbf{c}_u, \mathbf{x}_k \rangle}{\langle \mathbf{x}_k, \mathbf{x}_k \rangle} \mathbf{x}_k \right\|_2}, & u = 2, 3, \cdots, U, \end{cases} \tag{1}$$

where $\|\cdot\|_2$ and $\langle \cdot, \cdot \rangle$ are the 2-norm and inner product operations, respectively. After that, the u-th chaotic signal is extended by the discrete W vector $\mathbf{D}_u^R$ to form the u-th reference signal, i.e., $\mathbf{D}_u^R \otimes \mathbf{x}_u, u \in \{1, 2, \cdots, U\}$, where $\otimes$ is the Kronecker product and $\mathbf{D}_u^R \in \{\mathbf{D}_i\}_{i=1}^U$ is the u-th W vector in the R-branch. Note that $\mathbf{D}_i = [D_{i,1}, D_{i,2}, \cdots, D_{i,2N}]$ can be constructed by the discrete W transform, given by [15]

$$D_{i,j} = \sqrt{\frac{1}{N}} \sin\left(\frac{\pi}{4} + \frac{ij\pi}{N}\right), \; i, j \in \{1, 2, \cdots, 2N\}, \tag{2}$$

where $D_{i,j}$ is the j-th element of the i-th discrete W vector. According to [15], the $2N$ discrete W vectors, $\{\mathbf{D}_i\}_{i=1}^{2N}$, are orthogonal to each other.

Next, the U chaotic signals $\mathbf{X} = \{\mathbf{x}_1, \mathbf{x}_2, \cdots, \mathbf{x}_U\}$ and their orthogonal versions $\mathbf{Y} = \{\mathbf{y}_1, \mathbf{y}_2, \cdots, \mathbf{y}_U\}$ are loaded into the M-ary DCSK modulator to obtain the U M-ary signals. The u-th M-ary signal in the R-branch is $\mathbf{m}_{p,u}^R = a_{p,u}^R \mathbf{x}_u + b_{p,u}^R \mathbf{y}_u$, where $\mathbf{m}_{p,u}^R$ is a β-length row vector, $a_{p,u}^R$ and $b_{p,u}^R$ are real and imaginary components of the M-ary symbol. The modulation order is $M = 2^n$, where n is the number of transmitted bits per M-ary signal. After summing up the U M-ary signals and multiplying by $1/\sqrt{U}$, the p-th M-ary information-bearing signal in the R-branch is $\frac{1}{\sqrt{U}} \sum_{u=1}^U \mathbf{m}_{p,u}^R, p \in \{1, 2, \cdots, K_1\}$. Similarly, the q-th M-ary information-bearing signal in the I-branch is given by $\frac{1}{\sqrt{U}} \sum_{u=1}^U \mathbf{m}_{q,u}^I, q \in \{1, 2, \cdots, K_2\}$.

The resultant $K_1 + K_2$ M-ary signals are extended by the specific discrete W vectors $\{\mathbf{D}_p^F\}_{p=1}^{K_1}$ and $\{\mathbf{D}_q^I\}_{q=1}^{K_2}$, which are selected from the set $\{\mathbf{D}_i\}_{i=U+1}^N$ and $\{\mathbf{D}_i\}_{i=N+1}^{2N}$, respectively. A combination mapping method developed in [16] is used to achieve the index keying. Finally, the transmitted signal of the DWT-IK-MDCSK system is expressed as

$$\begin{aligned} \mathbf{T} = &\sum_{u=1}^{U} (\mathbf{D}_u^R \otimes \mathbf{x}_u) + \sum_{p=1}^{K_1} (\mathbf{D}_p^F \otimes \frac{1}{\sqrt{U}} \sum_{u=1}^{U} \mathbf{m}_{p,u}^R) \\ &+ \sqrt{-1} \sum_{q=1}^{K_2} (\mathbf{D}_q^I \otimes \frac{1}{\sqrt{U}} \sum_{u=1}^{U} \mathbf{m}_{q,u}^I). \end{aligned} \tag{3}$$

In the DWT-IK-MDCSK system, $\partial_1 = \lfloor \log_2(\binom{N-U}{K_1}) \rfloor$ and $\partial_2 = K_1 n U$ bits are the mapped bits and modulated bits in the R-branch, respectively, where $\binom{\cdot}{\cdot}$ and $\lfloor \cdot \rfloor$ represent the binomial coefficient and floor function. Then, $\partial_3 = \lfloor \log_2(\binom{N}{K_2}) \rfloor$ and $\partial_4 = K_2 n U$ are the mapped bits and modulated bits in the I-branch, respectively. Therefore, the total number of transmitted bits per DWT-IK-MDCSK symbol is calculated as $\partial = \lfloor \log_2(\binom{N-U}{K_1}) \rfloor + K_1 n U + \lfloor \log_2(\binom{N}{K_2}) \rfloor + K_2 n U$.

Considering an L-path Rayleigh fading channel, the received signal is $\mathbf{R} = \sum_{l=1}^L \alpha_l \mathbf{T}_{\tau_l} + \mathbf{n}$, where α_l and τ_l are the l-th path channel coefficient and time delay, respectively. In addition, $\mathbf{n} = \mathbf{n}^R + \sqrt{-1}\mathbf{n}^I$ is the complex AWGN, where $\mathbf{n}^R$ and $\mathbf{n}^I$ have zero mean and the power spectral density of $N_0/2$. The subscript τ_l is omitted in the sequel for brevity.

At the receiver, after extracting real and imaginary parts of the received signal, the resultant signals are multiplied by different discrete W vectors, i.e., $\mathbf{G}_i^R = \mathcal{R}(\mathbf{R}) \odot (\mathbf{D}_i \otimes \mathbf{1}_{1\times\beta})$ and $\mathbf{G}_i^I = \mathcal{I}(\mathbf{R}) \odot (\mathbf{D}_{i+N} \otimes \mathbf{1}_{1\times\beta}), i \in \{1, 2, \cdots, N\}$, where $\mathcal{R}(\cdot)$ and $\mathcal{I}(\cdot)$ return the real and imaginary parts. $\odot$ is the Hardamard product and $\mathbf{1}_{1\times\beta}$ is a β-length unit vector. Then, signals $\{\mathbf{G}_i^R\}_{i=1}^U$, $\{\mathbf{G}_i^R\}_{i=U+1}^N$ and $\{\mathbf{G}_i^I\}_{i=1}^N$ are averaged for every $2N$ elements to obtain the averaged reference and M-ary information-bearing signals, respectively. Therefore, the k-th averaged reference signal $\mathbf{G}_{ref,k}$ is given in (4), as shown at the bottom of next page. In Equation (4), $\text{Ave}\{\cdot\}_{2N}$ is the average operation for every $2N$ elements, and $\mathbf{n}_k$ is a β-length averaged AWGN with zero mean and $N_0/(4N)$ variance.

Similarly, the averaged information-bearing signals in the R- and I-branches are formulated, respectively, as

$$\mathbf{G}_{inf,k_1}^R = \sum_{l=1}^{L} \alpha_l [\frac{1}{\sqrt{U}} \sum_{u=1}^{U} (a_{k_1,u}^R \mathbf{x}_u + b_{k_1,u}^R \mathbf{y}_u)] + \mathbf{n}_{k_1}^R, \tag{5}$$

$$\mathbf{G}_{inf,k_2}^I = \sum_{l=1}^{L} \alpha_l [\frac{1}{\sqrt{U}} \sum_{u=1}^{U} (a_{k_2,u}^I \mathbf{x}_u + b_{k_2,u}^I \mathbf{y}_u)] + \mathbf{n}_{k_2}^I, \tag{6}$$

where $k_1 \in \{1, 2, \cdots, N-U\}$ and $k_2 \in \{1, 2, \cdots, N\}$. Then, $\mathbf{n}_{k_1}^R$ and $\mathbf{n}_{k_2}^I$ have the same means and variances as $\mathbf{n}_k$. The reference signals are stored in matrix $\mathbf{J}_x$, while the information-bearing signals in R- and I-branches are placed in matrices $\mathbf{A}$ and $\mathbf{B}$, respectively, expressed as $\mathbf{A} = [(\mathbf{G}_{inf,1}^R)^T, (\mathbf{G}_{inf,2}^R)^T, \cdots, (\mathbf{G}_{inf,N-U}^R)^T]_{\beta\times(N-U)}$ and

This article has been accepted for publication in a future issue of this journal, but has not been fully edited. Content may change prior to final publication. Citation information: DOI 10.1109/LCOMM.2021.3095075, IEEE Communications Letters

$\mathbf{B} = [(\mathbf{G}^I_{inf,1})^T, (\mathbf{G}^I_{inf,2})^T, \cdots, (\mathbf{G}^I_{inf,N})^T]_{\beta\times N}$, where $(\cdot)^T$ is the transposition operator. In addition, $\mathbf{J}_x$ and $\mathbf{J}_y$ in Fig. 1(b) are given by

$$\mathbf{J}_x = \left[\begin{array}{c} \mathbf{G}_{ref,1} \\ \vdots \\ \mathbf{G}_{ref,U} \end{array}\right]_{U\times\beta}, \quad \mathbf{J}_y = \left[\begin{array}{c} \tilde{\mathbf{G}}_{ref,1} \\ \vdots \\ \tilde{\mathbf{G}}_{ref,U} \end{array}\right]_{U\times\beta}, \tag{7}$$

where each row of $\mathbf{J}_y$ is orthogonal to that of $\mathbf{J}_x$.

To retrieve all information bits, the DWT-IK-MDCSK receiver not only needs to determine which discrete W vectors are selected to extend M-ary information-bearing signals and obtain the specific indices of these discrete W vectors, but also performs the M-ary DCSK demodulation to recover the modulated bits. First, $\mathbf{J}_x$ and $\mathbf{J}_y$ are multiplied by $\mathbf{A}$ or $\mathbf{B}$, respectively, yielding $\mathbf{Z}^R = \mathbf{J}_x\mathbf{A} + \sqrt{-1}\mathbf{J}_y\mathbf{A}$ and $\mathbf{Z}^I = \mathbf{J}_x\mathbf{B} + \sqrt{-1}\mathbf{J}_y\mathbf{B}$, which can be further deduced as (8) and (9), as shown at the bottom of this page.

After finding K_1 maximums from the set $\{|Z^R_{1,k_1}|\}^{N-U}_{k_1=1}$, where Z^R_{1,k_1} is the first row and k_1-th column of $\mathbf{Z}^R$, the indices of discrete W vectors are obtained and then the reverse combination mapping method [16] is used to regain ∂_1 mapped bits in the R-branch. Next, ∂_2 modulated bits in the R-branch are retrieved by using the M-ary DCSK demodulator. In the I-branch, ∂_3 mapped bits are retrieved by transforming K_2 selected indices of discrete W vectors, which are corresponding to K_2 maximum values selecting from the set $\{|Z^I_{1,k_2}|\}^{N}_{k_2=1}$, to the binary bits. After demodulating the M-ary information-bearing signals in the I-branch, the receiver finally estimates ∂_4 modulated bits.

III. Performance Analysis

Since the detection and demodulation in the R-branch are independent to those in the I-branch, we only need to evaluate the first row of the decision variable $\mathbf{Z}^R$ (i.e., Z^R_{1,k_1}) in the R-branch for brevity. When the indices of discrete W vectors are detected correctly, i.e., $k_1 = j$, the decision variable can be written as $Z^R_{1,j} = [(\sum_{l=1}^{L}\alpha_l\mathbf{x}_1 + \mathbf{n}_1) + \sqrt{-1}(\sum_{l=1}^{L}\alpha_l\mathbf{y}_1 + \tilde{\mathbf{n}}_1)][\sum_{l=1}^{L}\alpha_l(\frac{1}{\sqrt{U}}\sum_{u=1}^{U}(a^R_{j,u}\mathbf{x}_u + b^R_{j,u}\mathbf{y}_u)) + \mathbf{n}^R_j]^T$. Hence, the mean and variance of $Z^R_{1,j}$ are computed as

$$\begin{aligned}\mathrm{E}[Z^R_{1,j}] =& \mathrm{E}[\mathcal{R}(Z^R_{1,j})] + \mathrm{E}[\mathcal{I}(Z^R_{1,j})] = \mu_1 \\ =& \begin{cases} \frac{E_c}{\sqrt{U}}, & M = 2, \\ (a^R_{j,u} + b^R_{j,u})\frac{E_c}{\sqrt{U}}, & M > 2, \end{cases}\end{aligned} \tag{10}$$

$$\begin{aligned}\mathrm{Var}[Z^R_{1,j}] =& \mathrm{Var}[\mathcal{R}(Z^R_{1,j})] + \mathrm{Var}[\mathcal{I}(Z^R_{1,j})] = \sigma_1^2 \\ =& \begin{cases} \frac{E_cN_0}{2N} + \beta\frac{N_0^2}{16N^2}, & M = 2, \\ 2(\frac{E_cN_0}{2N} + \beta\frac{N_0^2}{16N^2}), & M > 2, \end{cases}\end{aligned} \tag{11}$$

where $\mathrm{E}[\cdot]$ and $\mathrm{Var}[\cdot]$ is mean and variance operations, respectively. Then, $E_c = \sum_{l=1}^{L}\alpha_l^2\mathrm{E}[\mathbf{x}_i(\mathbf{x}_i)^T], i \in \{1, 2, \cdots, U\}$ and the symbol energy of the DWT-IK-MDCSK system is computed as $E_s = 2N(U + K_1 + K_2)E_c$. Hence, the symbol signal-to-noise ratio (SNR) is given by $\gamma_s = \sum_{l=1}^{L}\alpha_l^2\frac{E_s}{N_0}$.

Considering the incorrect detection of discrete W vectors, namely $k_1 \neq j$, the decision variable can be given by $\hat{Z}^R_{1,k_1} = [(\sum_{l=1}^{L}\alpha_l\mathbf{x}_1 + \mathbf{n}_1) + \sqrt{-1}(\sum_{l=1}^{L}\alpha_l\mathbf{y}_1 + \tilde{\mathbf{n}}_1)][\mathbf{n}^R_{k_1}]^T$, whose mean and variance are calculated as

$$\mathrm{E}[\hat{Z}^R_{1,k_1}] = \mathrm{E}[\mathcal{R}(\hat{Z}^R_{1,k_1})] + \mathrm{E}[\mathcal{I}(\hat{Z}^R_{1,k_1})] = 0, \tag{12}$$

$$\begin{aligned}\mathrm{Var}[\hat{Z}^R_{1,k_1}] =& \mathrm{Var}[\mathcal{R}(\hat{Z}^R_{1,k_1})] + \mathrm{Var}[\mathcal{I}(\hat{Z}^R_{1,k_1})] = \sigma_2^2 \\ =& \begin{cases} \frac{E_cN_0}{4N} + \beta\frac{N_0^2}{16N^2}, & M = 2, \\ 2(\frac{E_cN_0}{4N} + \beta\frac{N_0^2}{16N^2}), & M > 2, \end{cases}\end{aligned} \tag{13}$$

When the minimum value of $\{|Z^R_{1,j}|\}^{K_1}_{j=1}$ is greater than the maximum value of $\{|\hat{Z}^R_{1,k_1}|\}^{N-U-K_1}_{k_1=1}$, the index detection of discrete W vectors in the R-branch is correct. Thus, the error probability of the index keying in the R-branch is [9], [17]

$$\begin{aligned}P^R_d =& \int_0^\infty \left\{1 - [F_\nu(t)]^\xi\right\}\psi[1 - F_\kappa(t)]^{\psi-1}f_\kappa(t)\mathrm{d}t \\ =& \mathbb{F}(\nu = |\hat{Z}^R_{1,k_1}|, \kappa = |Z^R_{1,j}|; \xi = N - U - K_1, \psi = K_1)\end{aligned} \tag{14}$$

where $f_\kappa(t) = \frac{1}{\sqrt{2\pi\sigma_1^2}}[\exp(-\frac{(t-\mu_1)^2}{2\sigma_1^2}) + \exp(-\frac{(t+\mu_1)^2}{2\sigma_1^2})]$ is the probability density function (PDF) of κ. Furthermore, $F_\nu(t)$ and $F_\kappa(t)$ are the cumulative distribution function (CDF) of ν and κ, respectively, formulated as $F_\nu(t) = \mathrm{erf}(\frac{t}{\sqrt{2\sigma_2^2}})$ and $F_\kappa(t) = \frac{1}{2}[\mathrm{erf}(\frac{t-\mu_1}{\sqrt{2\sigma_1^2}}) + \mathrm{erf}(\frac{t+\mu_1}{\sqrt{2\sigma_1^2}})]$. Here, $\mathrm{erf}(x) = \frac{2}{\sqrt{\pi}}\int_0^x e^{-t^2}\mathrm{d}t$ is the error function. In the I-branch, the error probability of the index keying is given

$$\mathbf{G}_{ref,k} = \mathrm{Ave}\left\{[\sum_{l=1}^{L}\alpha_l[\sum_{u=1}^{U}(\mathbf{D}^R_u \otimes \mathbf{x}_u) + \sum_{p=1}^{K_1}(\mathbf{D}^F_p \otimes \frac{1}{\sqrt{U}}\sum_{u=1}^{U}\mathbf{m}^R_{p,u})] + \mathbf{n}_R] \odot (\mathbf{D}_k \otimes \mathbf{1}_{1\times\beta})\right\}_{2N}$$
$$= \sum_{l=1}^{L}\alpha_l\mathbf{x}_k + \mathbf{n}_k, \quad k \in \{1, 2, \cdots, U\} \tag{4}$$

$$\mathbf{Z}^R = \left[\begin{array}{ccc} \mathbf{G}_{ref,1}(\mathbf{G}^R_{inf,1})^T & \cdots & \mathbf{G}_{ref,1}(\mathbf{G}^R_{inf,N-U})^T \\ \vdots & \ddots & \vdots \\ \mathbf{G}_{ref,U}(\mathbf{G}^R_{inf,1})^T & \cdots & \mathbf{G}_{ref,U}(\mathbf{G}^R_{inf,N-U})^T \end{array}\right] + \sqrt{-1}\left[\begin{array}{ccc} \tilde{\mathbf{G}}_{ref,1}(\mathbf{G}^R_{inf,1})^T & \cdots & \tilde{\mathbf{G}}_{ref,1}(\mathbf{G}^R_{inf,N-U})^T \\ \vdots & \ddots & \vdots \\ \tilde{\mathbf{G}}_{ref,U}(\mathbf{G}^R_{inf,1})^T & \cdots & \tilde{\mathbf{G}}_{ref,U}(\mathbf{G}^R_{inf,N-U})^T \end{array}\right] \tag{8}$$

$$\mathbf{Z}^I = \left[\begin{array}{ccc} \mathbf{G}_{ref,1}(\mathbf{G}^I_{inf,1})^T & \cdots & \mathbf{G}_{ref,1}(\mathbf{G}^I_{inf,N})^T \\ \vdots & \ddots & \vdots \\ \mathbf{G}_{ref,U}(\mathbf{G}^I_{inf,1})^T & \cdots & \mathbf{G}_{ref,U}(\mathbf{G}^I_{inf,N})^T \end{array}\right] + \sqrt{-1}\left[\begin{array}{ccc} \tilde{\mathbf{G}}_{ref,1}(\mathbf{G}^I_{inf,1})^T & \cdots & \tilde{\mathbf{G}}_{ref,1}(\mathbf{G}^I_{inf,N})^T \\ \vdots & \ddots & \vdots \\ \tilde{\mathbf{G}}_{ref,U}(\mathbf{G}^I_{inf,1})^T & \cdots & \tilde{\mathbf{G}}_{ref,U}(\mathbf{G}^I_{inf,N})^T \end{array}\right] \tag{9}$$

by $P_d^I = \mathbb{F}(\nu = |\hat{Z}_{1,k_2}^I|, \kappa = |Z_{1,j}^I|; \xi = N - K_2, \psi = K_2)$, where $\hat{Z}_{1,k_2}^I$ and $Z_{1,j}^I$ are the decision variables corresponding to the incorrect and correct index detections, respectively. In addition, $\hat{Z}_{1,k_2}^I$ and $Z_{1,j}^I$ have the same means and variances as $\hat{Z}_{1,k_1}^R$ and $Z_{1,j}^R$, respectively.

In the DWT-IK-MDCSK system, the demodulations of M-ary symbols in R- and I-branches are independent, and they have the same error probability, given by [18], [19]

$$P_e \approx \begin{cases} \frac{1}{2}\mathrm{erfc}[(\frac{2\mathrm{Var}[\mathcal{R}(Z_{1,j}^R)]}{(\mathrm{E}[\mathcal{R}(Z_{1,j}^R)])^2})^{-\frac{1}{2}}], & M = 2 \\ \frac{2}{n}Q(\frac{\mathrm{E}[\mathcal{R}(Z_{1,j}^R)]}{a_{j,u}^R\sqrt{\mathrm{Var}[\mathcal{R}(Z_{1,j}^R)]}}\sin\frac{\pi}{M}), & M > 2 \end{cases} \quad (15)$$

where $\mathrm{erfc}(x) = \frac{2}{\sqrt{\pi}}\int_x^\infty e^{-t^2}\mathrm{d}t$ is the complementary error function and $Q(x) = \frac{1}{\sqrt{2\pi}}\int_x^\infty \exp(-\frac{t^2}{2})\mathrm{d}t, x \geq 0$.

According to the probability theory, the total BER of the DWT-IK-MDCSK system can be formulated as $P_T = \frac{\partial_1}{\partial}P_{map}^R + \frac{\partial_2}{\partial}P_{mod}^R + \frac{\partial_3}{\partial}P_{map}^I + \frac{\partial_4}{\partial}P_{mod}^I$, where P_{map}^R and P_{mod}^R are the BERs of mapped bits and modulated bits in the R-branch, while P_{map}^I and P_{mod}^I are the BERs of mapped bits and modulated bits in the I-branch. The aforementioned BERs can be obtained as [20], [21] $P_{map}^R = \frac{2^{\partial_1-1}}{2^{\partial_1}-1}P_d^R$, $P_{mod}^R = (1-P_d^R) + P_\Omega^R P_e$, $P_{map}^I = \frac{2^{\partial_3-1}}{2^{\partial_3}-1}P_d^I$ and $P_{mod}^I = (1-P_d^I) + P_\Omega^I P_e$, respectively, where $P_\Omega^R = \frac{1}{K_1\sum_{i=1}^{K_1}\binom{K_1}{i}}\sum_{i=1}^{K_1}\binom{K_1}{i}[\frac{i}{2} + (K_1 - i)P_e] = \mathbb{P}(K_1)$ and $P_\Omega^I = \mathbb{P}(K_2)$. Considering the multipath Rayleigh fading channel, the BER of the DWT-IK-MDCSK system is expressed as $\bar{P}_T = \int_0^\infty P_T(\gamma_s)\cdot f(\gamma_s)\mathrm{d}\gamma_s$, where $f(\gamma_s) = \sum_{l=1}^L[\frac{1}{\bar{\gamma}_l}(\prod_{j=1,j\neq l}^L\frac{\bar{\gamma}_l}{\bar{\gamma}_l - \bar{\gamma}_j})\exp(-\frac{\gamma_s}{\bar{\gamma}_l})]$ is the PDF of symbol-SNR γ_s and $\bar{\gamma}_l$ is the average SNR of the l-th path[1].

IV. Numerical Results and Discussions

Define the total number of transmitted bits per symbol as the data rate. According to [7], [8], the data rates of the DCS-MDCSK and MCS-MDCSK systems are $\partial_D = U(2N - U)$ and $\partial_M = n\lfloor\frac{N-1}{2}\rfloor$, respectively. Fig. 2 is plotted to compare the data rates of different systems. Clearly, the DWT-IK-MDCSK system has a higher data rate than its competitors.

The number of spreading and despreading operations is used to evaluate the computation complexity (CC). Table I shows the system complexities of the DWT-IK-MDCSK and other systems under the condition of the same data rate. In Table I, $U = 1, K_1 = 2, K_2 = 3$ and $M = 2$ are used in the DWT-IK-MDCSK system. When $\partial = 10$ and 12, the DWT-IK-MDCSK system uses $N = 5$ and $N = 6$, respectively. $N = 4$ and $U = 2$ are used in the DCS-MDCSK system, while $M = 4$ and the order of Walsh codes $N_w = 4$ are used in the CIM-MC-MDCSK system. According to Table I, the system complexity of the DWT-IK-MDCSK system is higher than the CIM-MC-MDCSK system, but lower than the DCS-MDCSK system.

The complementary cumulative distribution function (CCDF), defined by $CCDF = \Pr(PAPR > PAPR_0)$, is used to evaluate the PAPR performance, where $PAPR = \frac{\max(|T_k|^2)}{\mathrm{E}(|T_k|^2)}$ and $PAPR_0$ is a given PAPR threshold. In Fig. 2, the PAPR performance of the DWT-IK-MDCSK system is compared to its competitors under the condition of the same data rate. The simulation parameters are the same as that of Table I. When $\partial = 34$, the system parameters $N = 32, U = 1, K_1 = 3, K_2 = 4$ and $M = 2$ are used in the simulation of DWT-IK-MDCSK. In CIM-MCS-DCSK, the order of Walsh code is set to 32 and the number of parallel information-bearing branches is set to 4. Therefore, the data rate of CIM-MCS-DCSK is obtained as $\partial_F = 34$. Clearly, DWT-IK-MDCSK achieves about 2dB and 6dB PAPR performance gains compared to the DCS-MDCSK and CIM-MC-MDCSK systems, respectively, at 10^{-4} CCDF level. In addition, the PAPR performance of DWT-IK-MDCSK outperforms CIM-MCS-DCSK and the gain is about 1dB.

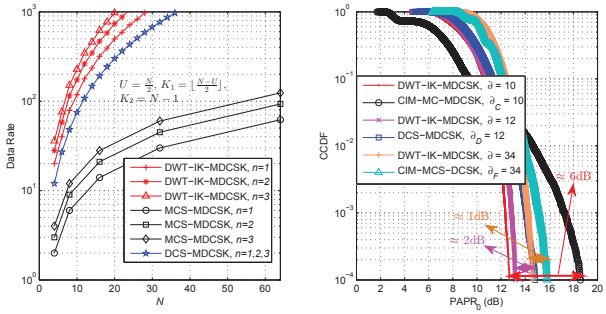

Fig. 2. Data rate comparison (left one) and PAPR performance comparison, $\beta = 100$ (right one).

TABLE I
Comparison of System Complexity

Data rate	System	CC	Hilbert filter	Matched filter
$\partial = 10$	DWT-IK-MDCSK	18	✓	×
	CIM-MC-MDCSK	16	✓	✓
$\partial = 12$	DWT-IK-MDCSK	20	✓	×
	DCS-MDCSK	24	×	✓

In simulations, a three-path Rayleigh fading channel with power coefficients $\mathrm{E}(\alpha_1^2) = 4/7, \mathrm{E}(\alpha_2^2) = 2/7, \mathrm{E}(\alpha_3^2) = 1/7$ and delay times $\tau_1 = 0, \tau_2 = 2T_c, \tau_3 = 4T_c$ is used, where T_c is the chip duration. "Simu" and "Ana" denote simulation and analytical results, respectively.

As shown in Fig. 3, when U is kept constant and β is increased (or β is kept constant and U is increased), the BER performance of DWT-IK-MDCSK becomes worse and worse. Fig. 4 suggests the DWT-IK-MDCSK system achieves the best BER performance when $M = 4$ and $K_1 = K_2 = 1$. The DWT-IK-MDCSK system shows a deteriorating BER performance when K_1 and K_2 are increased, because the error probability of the detection for the index keying is increased with large K_1 and K_2. Furthermore, simulation results match the analytical ones, verifying the correctness of our derivations.

Fig. 5 shows the BER performances of DWT-IK-MDCSK and other chaotic communication systems. In the DWT-IK-MDCSK system, $U = 1, N = 5, K_1 = K_2 = 1$ and $M = 4$. Then, $N = 3$ and $U = 2$ are applied in the DCS-MDCSK system. The MCS-MDCSK system uses $U_t = 7$ and $M = 2$ in simulations, where U_t is the number of parallel M-ary information-bearing signals. In the CIM-MC-MDCSK system, $M = 2$ and $N_w = 4$ is used, and its data rate is $\partial_C = 6$. As observed in Fig. 5, the proposed DWT-

[1]Due to the limited space, the closed-form BER is not given here. If someone is interested in the closed-form solutions, please refer to [4] and [19].

This article has been accepted for publication in a future issue of this journal, but has not been fully edited. Content may change prior to final publication. Citation information: DOI 10.1109/LCOMM.2021.3095075, IEEE Communications Letters

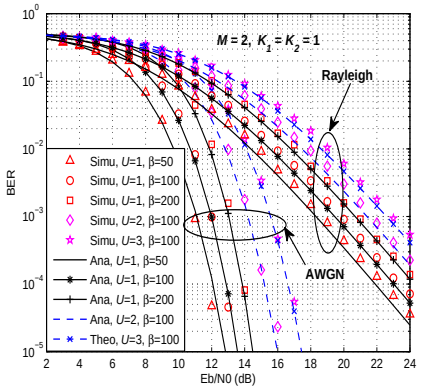

Fig. 3. BER of the DWT-IK-MDCSK system with various U and β.

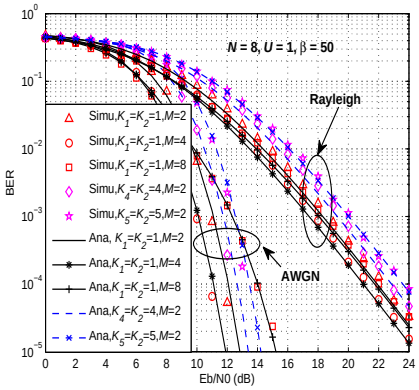

Fig. 4. BER of the DWT-IK-MDCSK system with various K_1, K_2 and M.

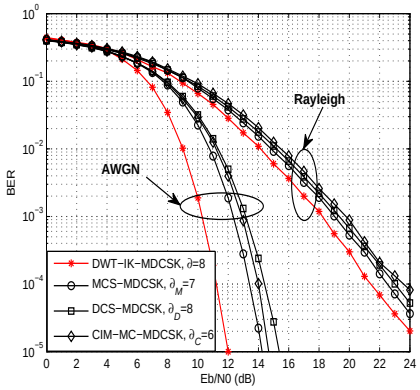

Fig. 5. BER performance comparison, $\beta = 50$.

IK-MDCSK system achieves the best BER performance in contrast to its competitors. Particularly, the DWT-IK-MDCSK system obtains more than 2dB performance gain over the MCS-MDCSK system and 3.5dB gain over the DCS-MDCSK system at the BER level 10^{-5} in the AWGN channel.

V. Conclusion

A non-coherent discrete W transform based index-keying M-ary differential chaos shift keying system has been proposed in this paper. In the system, the index keying is used to determine which discrete W vectors are used for information transmission. Since extra bits are conveyed by the indices of discrete W vectors, the DWT-IK-MDCSK system achieves a higher data rate. In addition, the DWT-IK-MDCSK system is more flexible and practical than traditional CIM-based DCSK system, as the order of the discrete W vector can be any integer greater than 1. Then, the BER expressions of the DWT-IK-MDCSK system are derived, which have been checked by computer simulations. Simulation results have shown that the DWT-IK-MDCSK system obtains 2 to 3.5dB BER performance gain and 1 to 6dB PAPR performance gain compared to other chaotic communication systems.

References

[1] M. R. Palattella *et al.*, "Internet of things in the 5G era: Enablers, architecture, and business models," *IEEE J. Sel. Areas Commun.,*, vol. 34, no. 3, pp. 510-527, March 2016.

[2] M. Qian, G. Cai, Y. Fang and G. Han, "Design of link-selection strategies for buffer-aided DCSK-SWIPT relay system," *IEEE Trans. Commun.*, vol. 68, no. 10, pp. 6023-6038, Oct. 2020.

[3] G. Kolumbán, G. K. Vizvári, W. Schwarz, and A. Abel, "Differential chaos shift keying: A robust coding for chaos communication," in *Proc. Nonlinear Dyn. Electron. Syst.*, Seville, Spain, 1996, pp. 92-97.

[4] G. Cai and Y. Song, "Closed-form BER expressions of M-ary DCSK systems over multipath Rayleigh fading channels," *IEEE Commun. Lett.*, vol. 24, no. 6, pp. 1192-1196, June 2020.

[5] Y. Fang, G. Han, P. Chen, F. C. M. Lau, G. Chen and L. Wang, "A survey on DCSK-based communication systems and their application to UWB scenarios," *IEEE Commun. Survey Tutor.*, vol. 18, no. 3, pp. 1804-1837, third quarter 2016.

[6] L. Wang, G. Cai, and G. R. Chen, "Design and performance analysis of a new multiresolution M-ary differential chaos shift keying communication system," *IEEE Trans. Wireless Commun.*, vol. 14, no. 9, pp. 5197-5208, Sep. 2015.

[7] X. Cai, W. Xu, R. Zhang, and L. Wang, "A multilevel code shifted differential chaos shift keying system with M-ary modulation," *IEEE Trans. Circuits Syst. II, Exp. Briefs*, vol. 66, no. 8, pp. 1451-1455, Aug. 2019.

[8] Z. Chen, L. Zhang and Z. Wu, "High data rate discrete-cosine-spreading aided M-ary differential chaos shift keying scheme with low PAPR," *IEEE Trans. Circuits Syst. II, Exp. Briefs*, vol. 67, no. 11, pp. 2492-2496, Nov. 2020.

[9] G. Kaddoum, Y. Nijsure, and H. Tran, "Generalized code index modulation technique for high-data-rate communication systems," *IEEE Trans. Veh. Technol.*, vol. 65, no. 9, pp. 7000-7009, Sep. 2016.

[10] E. Aydin, F. Cogen and E. Basar, "Code-index modulation aided quadrature spatial modulation for high-rate MIMO systems," *IEEE Trans. Veh. Tech.*, vol. 68, no. 10, pp. 10257-10261, Oct. 2019.

[11] Q. Li, M. Wen, E. Basar, and F. Chen, "Index modulated OFDM spread spectrum," *IEEE Trans. Wireless Commun.*, vol. 17, no. 4, pp. 2360-2374, Apr. 2018.

[12] Y. Tan, W. Xu, T. Huang and L. Wang, "A multilevel code shifted differential chaos shift keying scheme with code index modulation," *IEEE Trans. Circuits Syst. II, Exp. Briefs*, vol. 65, no. 11, pp. 1743-1747, Nov. 2018.

[13] G. Cai, Y. Fang, J. Wen, S. Mumtaz, Y. Song and V. Frascolla, "Multi-carrier M-ary DCSK system with code index modulation: An efficient solution for chaotic communications," *IEEE J. Sel. Topics Signal Process.*, vol. 13, no. 6, pp. 1375-1386, Oct. 2019.

[14] G. Cai, Y. Fang, P. Chen, G. Han, G. Cai and Y. Song, "Design of an MISO-SWIPT-aided code-index modulated multi-carrier M-DCSK system for e-health IoT," *IEEE J. Sel. Areas Commun.*, vol. 39, no. 2, pp. 311-324, Feb. 2021.

[15] Z. Wang, "Fast algorithms for the discrete W transform and for the discrete Fourier transform," *IEEE Trans. Acoust., Speech, Signal Processing*, vol. ASSP-32, pp. 803-816, Apr. 1984.

[16] E. Başar, Ü. Aygölü, E. Panayırcı and H. V. Poor, "Orthogonal frequency division multiplexing with index modulation," *IEEE Trans Signal Process.*, vol. 61, no. 22, pp. 5536-5549, Nov.15, 2013.

[17] X. Cai, W. Xu, F. C. M. Lau and L. Wang, "Joint carrier-code index modulation aided M-ary differential chaos shift keying system," *IEEE Trans. Veh. Technol.* vol. 69, no. 12, pp. 15486-15499, Dec. 2020.

[18] X. Cai, W. Xu, D. Wang, S. Hong and L. Wang, "An M-ary orthogonal multilevel differential chaos shift keying system with code index modulation," *IEEE Trans. Commun.*, vol. 67, no. 7, pp. 4835-4847, July 2019.

[19] M. Dawa, G. Kaddoum and Z. Sattar, "A generalized lower bound on the bit error rate of DCSK systems over multi-path Rayleigh fading channels," *IEEE Trans. Circuits Syst. II, Exp. Briefs*, vol. 65, no. 3, pp. 321-325, March 2018.

[20] X. Cai, W. Xu, L. Wang and G. Chen, "Towards high-data-rate noncoherent chaotic communication: A multiple-mode differential chaos shift keying system," *IEEE Trans. Wireless Commun.* doi: 10.1109/TWC.2021.3062836.

[21] H. Ma, G. Cai, Y. Fang, P. Chen and G. Chen, "Design of a superposition coding PPM-DCSK system for downlink multi-user transmission," *IEEE Trans. Veh. Technol.*, vol. 69, no. 2, pp. 1666-1678, Feb. 2020.